8. G. K. Batchelor, Introduction to Fluid Dynamics, Cambridge Univ. Press, New York (1967).
9. H. H. Legner, "A simple model for gas bubble drag reduction," Phys. Fluids, 27, No. 12 (1984).
10. A. Biesheuvel and L. Wijngaarden, "Two-phase flow equations for a dilute dispersion of gas bubbles in liquid," J. Fluid. Mech., 148, 301 (1984).
11. M. Severa and J. Hrbek, "Viscosity of suspensions formulated on the basis of the theory of dissipative disperse systems," in: Rheology and Rheometry of Multiphase Liquid Systems [in Czech], Hydrodyn. Inst., Czech. Acad. Sci., Prague (1979).
12. F. Eirich (ed.), Rheology: Theory and Applications, 5 vols., Academic Press, New York (1956-1969).
13. S. K. Godunov, Elements of Solid Material Mechanics [in Russian], Nauka, Moscow (1978).

# SHOCK-INDUCED CONDUCTION WAVES IN ELECTROPHYSICAL EXPERIMENTS

E. I. Bichenkov, S. D. Gilev, and A. M. Trubachev

UDC 621.3:539.89:537.311.3

## 1. SHOCK WAVES AND ELECTROPHYSICAL EXPERIMENTS. INTRODUCTORY REMARKS

Research and practical developments in controlled thermonuclear fusion and the preparation of new materials with unique properties require high energy densities, necessary for overcoming activation barriers of the corresponding chemical or nuclear reactions, in the material. The solution of these problems led to the creation and rapid development, during the last 10 years, of a new field of scientific research – the physics of high-energy densities, associated with the creation and control of extremely high energy fluxes in powerful, predominantly pulsed, energy systems [1]. Because of the extensive possibilities for conversion of energy into other forms and for transformation, storage, and transfer of energy, sources of electromagnetic energy operating with currents of $10^6$-$10^8$ A, magnetic fields of $10^2$-$10^3$ T, voltages of $10^4$-$10^6$ V, energies of $10^5$-$10^7$ J over times from several nanoseconds to tens of microseconds, and powers of up to $10^{13}$ W and higher [2-6] have been predominantly developed.

The energy flux in powerful electric circuits is controlled with the help of elements with variable electrotechnical parameters (most often the inductance and resistance). The inductance is determined by the geometric characteristics of the conductors, and the possibilities for changing it rapidly are limited. The resistance expresses both the geometric ratios of a section of the circuit and the physical properties of the state of the matter and can be changed substantially by strong, external actions. This is of great significance for practical applications in pulsed systems (switches operating based on the most diverse physical principles). The main problems in the operation of switching elements are associated with the operation of switching the current off. Thus, the parameters of a switch for interrupting the current in an inductive storage circuit determine the applications of this promising source of energy [7].

The physical properties of matter can be altered by different external actions, such as heating, radiation, electrical breakdown, etc. Among such actions high pressure and the concomitant strong compression of matter stand out especially, since under these conditions the electrical properties change radically. The study of the electric conductivity of materials at high pressure was initiated by Bridgman [8]. Significant progress has now been achieved in this field [9-17]. Progress in research on the electric properties of materials at high pressure is linked with improvement of the measuring technology and the good status of the physical theory, which is sufficient for giving a satisfactory description of the phenomena occurring in some "pure" cases.

Sharp changes in the electric conductivity of condensed materials, induced by powerful shock waves (SWs) and accompanied by the appearance or vanishing of metallic conductivity,

Novosibirsk. Translated from Zhurnal Prikladnoi Mekhaniki i Tekhnicheskoi Fiziki, No. 2, pp. 132-145, March-April, 1989. Original article submitted August 3, 1988.

0021-8944/89/3002-0291$12.50 

present a number of interesting possibilities for practical applications in systems for transmitting and converting electromagnetic energy. This paper is devoted to the study of such transitions as well as their application for switching currents and obtaining superstrong magnetic fields.

Physical Processes in SWs. There are several physical processes that are accompanied by a sharp change in the electric conductivity.

1. Polymorphic transition. This transition is of a threshold character and occurs when conditions such that the starting crystalline structure becomes unstable and the material transforms into a new structural state are reached. The transition time is determined by the displacement of an atom in a crystalline cell. When the pressure is removed, the material returns into the starting crystalline state or a state close to it. The macroscopic state of the sample exposed to SWs differs from the starting state by the sizes of the microcrystals and the high degree of defectiveness.

2. Metallization of the material. A decrease in the interatomic spacing due to compression is accompanied by broadening of the energy bands and decrease of the energy gap between the valence and conduction bands. For some level of compression the gap vanishes — a transition of the material into a metallic phase occurs. The transition time is determined by the time required for the atoms to move over a distance of the order of the interatomic spacing. The transition is not always reversible: when the pressure is removed, the metallic phase can remain in the metastable state, if an appreciable activation barrier separates it from the starting state and the residual temperature of the sample is low.

3. Electronic transition. The compression of some materials characterized by anomalies in the sequence of occupation of the electronic energy levels changes the order of occupation of the energy bands, as a result of which electrons are redistributed between the bands and the conduction band is depopulated, i.e., the conduction of such materials at a certain degree of compression drops and these materials can transform into a semiconductor with the characteristic temperature dependence of the electric conductivity and the existence of impurities and structural defects. Further compression ultimately leads to metallization and an increase in the electric conductivity. The transition time is of the same order of magnitude as in preceding cases. Satisfactory reversibility of the transition with an accuracy up to possible heating and accumulation of structural defects should be expected.

These transitions accompanied by a sharp change in the electric conductivity depend primarily on the compression and are observed in a pure form when the pressure is applied in a quasistatic fashion. In SWs they become more complicated due to the unavoidable heating, whose magnitude is all the higher the greater the compression. Aside from the transitions enumerated above, transitions that are more characteristic for shock compression are also observed.

4. Change in the aggregate state of the material. With shock compression of low-density materials heating can lead to melting and even vaporization accompanied by a transition of the material into dense, nonconducting vapor either during the compression process or during the subsequent expansion process [11]. The transition time is determined primarily by the gasdynamics of the compression and rarefaction wave. The transition is irreversible.

5. Change in the chemical composition accompanied by formation of conducting products during a definite phase of the process and subsequent change in the conductivity in accordance with the thermodynamic state and composition of the products of transformation [18].

The possibilities enumerated above for a strong compression-induced change in the electric conductivity of materials are determined by the change in the internal structure of the materials at atomic or molecular levels. A broader view of the problem permits adding to the foregoing process the following.

6. Change in the morphological characteristics of heterogeneous materials. It is possible to make a composite material from highly conducting particles coated with a thin layer of dielectric. In the starting state such a material will be nonconducting. Compression destroys the insulating layer and good conductivity arises. The transition time is determined by the sum of the time for rupturing the dielectric and the time for the skin effect to form in the conducting particle. A morphological transition is obviously irreversible.

Examples of Transitions and Their Physical Characteristics. The most interesting shock-induced transitions accompanied by a sharp change in the conductivity are enumerated

TABLE 1

| Transition | Material | $p_{tr}$, GPa | $\sigma_0$, $\Omega^{-1} \cdot m^{-1}$ | $\sigma$, $\Omega^{-1} \cdot m^{-1}$ |
|---|---|---|---|---|
| Metal–metal | Fe | ~10 | $\sim 10^7$ | $\sim 10^7$ |
| Dielectric–semiconductor | $CCl_4$, NaCl | ~10 | $\sim 10^{-10}$ | $\sim 10^2$ |
| Dielectric (semiconductor)–metal | S, Si | ~10 | $\sim 10^{-10}$—$10^2$ | $\sim 10^7$ |
| Metal–semiconductor (dielectric) | Yb, Sr | ~2 | $\sim 10^7$ | $\sim 10^3$ |

in Table 1, which gives examples of materials undergoing the indicated transition, the order of magnitude of the transition pressures $p_{tr}$, and the limits of variation of the electric conductivity $\sigma$. The published transition times do not exceed $\sim 10^{-7}$ sec. We call attention to the characteristic features of the transitions given in the table.

1. The metal–metal transition is distinguished by the small change in the electric conductivity. For all metals resistance owing primarily to shock-induced heating and increase in the number of defects is observed. Owing to the absence of a temperature component it was of significant interest to study the pressure dependence of the resistance of manganin; this is used for measuring pulsed pressures in almost a megabar range [9]. It is difficult to overestimate the significance of this for shock-wave experiments.

2. The dielectric (semiconductor)–metal transition, which is understood best, has a general character and is typical for dielectrics. The phase transition pressure is proportional to the width of the energy gap. The change in the conductivity is sharpest for this transition and reaches 20 orders of magnitude. The difficulties in recording the transition are associated with the large jump in the conductivity and the high rate of the transition. We shall refer the transition associated with a change in the morphology of heterogeneous media to transitions of this type.

3. The metal–semiconductor (dielectric) transition, owing to its exotic nature, is observed for a small number of not very common elements and compounds in a quite narrow pressure range. At the present time, in connection with the discovery of high-temperature superconductivity in ceramic materials consisting of complex oxides, a transition in SWs whose outward manifestations are close to that of a metal–dielectric transition should be expected.

All transitions enumerated in Table 1 can be employed to one or another degree in electrophysical experiments. Since in strong-current circuits a positive effect is associated directly with the sharpness of the change in the conductivity of the material and with the quite high value of the conductivity in one of the states the dielectric–metal and metal–semiconductor transitions are of greatest interest.

## 2. INVESTIGATION OF THE CHANGE IN THE ELECTRIC CONDUCTIVITY OF METALS IN AN SW. DIELECTRIC (SEMICONDUCTOR)–METAL PHASE TRANSITION

1. The main problem in the experimental study of this transition in SWs is to measure a jump in $\sigma$ by several orders of magnitude with the final value corresponding to that of standard metals over a time much shorter than 1 μsec. Over the quarter century since the research was initiated, two basic schemes for measuring the electric conductivity had been developed and are now recognized [20]: the constant voltage method, employed for measuring relatively low conductivity, and the dc method for measuring high conductivity. To study transitions into a highly conducting state, the dc scheme with an additional shunt, connected in parallel to the sample and serving to limit the signal, must be employed [21-25]. Adequate measurement accuracy can be achieved if the resolution time of the shunt–sample measuring circuit, consisting of an inductance L and resistance R, $\tau = L/R$, is shorter than the time for which the high pressure exists. However, because the shunt and sample are spatially separated, the inductance of the measuring cell is appreciable, which for short SW action times leads to an upper limit for the measured conductivity [13, 20, 26]. The limiting values equal $\sim 10^4\ \Omega^{-1} \cdot m^{-1}$ for single shock compression and $\sim 10^5\ \Omega^{-1} \cdot m^{-1}$ for repeated shock compression. Comparing these quantities with the parameters in Table 1, it is obvious that to record a transition into the metallic state the resolution must be increased by two orders of magnitude. This can be done by changing the construction of the measuring cell and decreasing its inductance to the minimum value. The best procedure is to prepare a shunt

in the form of wide and thin strips of metallic foil placed directly on the surface of the sample under study. The shock wave enters the sample through the shunt. In the process the current initially flowing along the shunt is redistributed between the shunt and the part of the sample subjected to compression. This process has the character of a diffusion current, created by the propagating SW, from the surface layer into the bulk of the conductor and the measurement method can be further improved only by taking into account the dynamics of the growth of the skin layer under the conditions of shock-induced transition of the material into the conducting state. Careful referencing of the calculation of the nonstationary diffusion current to measurements of the voltage at the shunt–sample interface, measured with electrodes placed in the interface, is the second important feature of the measurement method which we have developed, a particular case of which, referring to a weak skin effect, is described in [27, 28]. Finally, in order to increase the accuracy of measurements of small resistances, it was necessary to raise the current in the measuring cell up to 700 A, which is more than an order of magnitude higher than the currents employed by other authors.

2. Comparison of the calculation of the nonstationary diffusion current flowing out of the shunt into the sample and measurement of the voltage on the shunt–sample boundary plays a very important role in the proposed method. For the flat geometry chosen the problem can be formulated as follows. In the region occupied by the shunt ($-1 \leq \xi \leq 0$), the magnetic field satisfies the equation

$$\frac{\partial b_1}{\partial \tau} - \frac{1}{\mathrm{Re}_m}\frac{\partial^2 b_1}{\partial \xi^2} = 0; \tag{2.1}$$

and in the sample ($0 \leq \xi \leq x_0/x_1$)

$$\frac{\partial b_2}{\partial \tau} - \frac{1}{\mathrm{Re}_m s}\frac{\partial^2 b_2}{\partial \xi^2} = 0. \tag{2.2}$$

Here the field is scaled to the starting value $B_0$ on the outer surface of the shunt, the spatial dimensions are scaled to the thickness of the shunt $x_1$, and the time is scaled to the passage time of the SW in the material of the layer with thickness $x_1$, i.e.,

$$b = B/B_0,\ \xi = x/x_1,\ \tau = t/t_0,\ t_0 = x_1/D. \tag{2.3}$$

Two parameters are important in the problem: the magnetic Reynolds number

$$\mathrm{Re}_m = \mu_0 \sigma_1 D x_1, \tag{2.4}$$

determined by the thickness of the shunt $x_1$ and its conductivity $\sigma_1$, and the ratio of the conductivities of the shunt and of the material

$$s = \sigma/\sigma_1. \tag{2.5}$$

The conductivity $\sigma$ of the material behind the SW front is assumed to be constant. Constancy of the current in the circuit leads to the boundary conditions

$$b_1(-1, \tau) = 1 \tag{2.6}$$

on the outer surface of the shunt and

$$b_2(\tau(1 - u/D), \tau) = -1, \quad \tau \leqslant x_0/x_1 \tag{2.7}$$

on the SW front (D and u are the wave and mass velocity in the material).

Continuity of the electric and magnetic fields on the shunt-material contact boundary leads to

$$\partial b_1/\partial \xi|_{\xi=0} = s\partial b_2/\partial \xi|_{\xi=0}; \tag{2.8}$$

$$b_1(0, \tau) = b_2(0, \tau). \tag{2.9}$$

The initial conditions are obvious:

$$b_1(\xi, 0) = -1 - 2\xi, \quad b_2(\xi, 0) = -1. \tag{2.10}$$

The voltage V(t) displayed on an oscillograph was identified with a quantity proportional to $\partial b_1/\partial \xi\big|_{\xi=0}$.

The formulated problem (2.1), (2.2) and (2.6)-(2.10) was solved numerically. It was established for several model cases that the magnitude and distribution of the currents in the material depend strongly on the dimensionless parameter

$$r = \mu_0 \sigma D^2 t (1 - u/D)^2. \tag{2.11}$$

If $r \ll 1$, there is no skin effect in the sample and the current simply follows immediately behind the SW in the compressed material. For $r \simeq 1$ the skin effect becomes appreciable, and for $r \gtrsim 10$ the SW detaches from the skin layer and the current distribution in the sample becomes strongly nonuniform.

The problem of determining the unknown $\sigma$ is the inverse of the problem of diffusion of the magnetic field formulated above. It was solved by comparing the diffusion $\partial b_1/\partial \xi\big|_{\xi=0}$ calculated in the problem with the experimental dependence V(t) and by adjusting $\sigma$ until the best agreement between these values taking into account the required normalizations is achieved. The accuracy with which $\sigma$ is determined was evaluated by the standard method of varying it by ±10-15% and by comparing the deviation of the corresponding computed voltage curves from the experimental values.

The case when the skin effect is unimportant is the simplest one to analyze. In this case it may be assumed that the current distribution both in the shunt and in the material behind the SW is uniform and simple calculations give the dependence V(t) in the form

$$\frac{V_0}{V(t)} = 1 + \frac{\sigma}{\sigma_1}\frac{(D-u)}{x_1}t, \tag{2.12}$$

which opens up the convenient possibility of rescaling the experimental curve V(t) to the coordinates $(V_0/V - 1, t)$ and determining $\sigma$ based on the slope of the straight line obtained.

In finishing the description of our method for measuring the conductivity we emphasize its basic advantages: 1) the simple geometry of the measurement cell permits analyzing accurately the transient processes occurring in it, reducing them to the classical problem of the skin effect in a conductor, and thereby determining reliably the electric conductivity under the conditions of propagation of an SW along the sample from the material studied, increasing both the accuracy in determining $\sigma$ and the time resolution: 2) in the process the agreement of the oscillogram V(t) with the computed curve is analyzed on the maximum time interval, unlike the results of [21, 23-25] which were obtained based on one point of the oscillogram corresponding to the minimum signal; and, 3) by determining the appropriate resistance of the shunt and current in the measurement cell it was possible to obtain reliable measurements of the electric conductivity of the order of the conductivity of good metals. The possibilities of the measurement method were evaluated in control experiments, when constantan and copper were employed as the materials studied.

The measurement method developed has certain restrictions associated with the placement of the shunt between the source of the SW and the sample and the microscopic characteristics of the shunt–sample contact. Because of reverberation of the SW arising at the shunt–sample boundary the pressure in the sample grew over a period of time determined by the ratio of the wave impedances of the materials and the thickness of the shunt. For shunt thicknesses of ~100 μm usually employed in our experiments, the shock-wave establishment time was about 100 nsec. This led to two restrictions: 1) the structure of the conducting zone on the wavefront could not be resolved and 2) the conductivities measured with good accuracy had an upper limit of $\sigma_* \simeq 1.2 \cdot 10^7\ \Omega^{-1} \cdot m^{-1}$. These restrictions can be completely removed by matching the shock impedances of the shunt and the sample. The unavoidable roughness of the contact leads, however, to local heating and nonuniformity of the electric contact of the two conductors, which in its turn will be reflected in the flow of current into the material studied and will be superposed on the transition of the sample into the conducting state.

The pressure in the measuring cell was calculated based on measurement of the wave velocity and the known shock adiabats of materials [16] and was monitored independently with a manganin sensor. Getinaks was employed as the insulation material, since unlike other commonly used plastics it does not give polarization signals induced by strong SWs.

3. An oscillogram of the experiment on measuring the conductivity of porous silicon and the results of its rescaling to the variables $(V_0/V - 1, t)$ are presented in Fig. 1a. It is obvious that the experiment agrees well with the assumption that the conductivity after

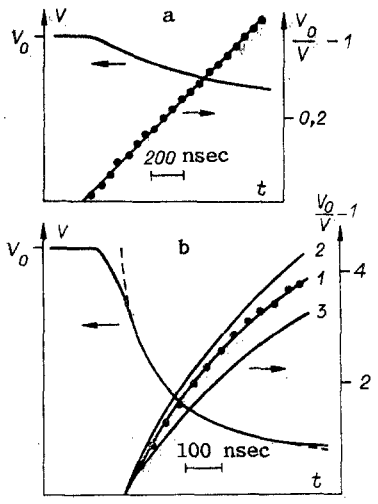


Fig. 1

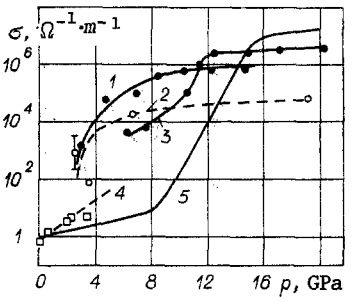


Fig. 2

shock compression is constant and that there is virtually no skin effect. The experiment corresponds to a conductivity of $6 \cdot 10^4$ $\Omega^{-1} \cdot m^{-1}$ and a pressure of 4.6 GPa. Numerical estimates for the conductivity, when the skin effect is insignificant, give $\sigma < 10^5$ $\Omega^{-1} \cdot m^{-1}$, which corresponds to the experimental results obtained.

The data from one experiment with large compression of porous silicon and high expected electric conductivities are shown in Fig. 1b. The oscillogram of the experiment was also rescaled to the variables $(V_0/V - 1, t)$ (dots). Curve 1 was computed with $\sigma = 9 \cdot 10^5$ $\Omega^{-1} \cdot m^{-1}$. The corresponding computed dependence V(t) is shown by the broken line and agrees well with the oscillogram, except for the starting section corresponding to the establishment of the pressure in the shunt by the shock wave. The accuracy with which σ is reconstructed can be judged from curves 2 and 3, which were computed for values of the conductivity differing from the values found by ±15%.

4. Quite detailed measurements of the electric conductivity of a number of materials which undergo an SW-induced transition into the conducting state were performed by the method described above. The experimental results obtained with silicon are presented in Fig. 2, where curve 1 shows the data from about 20 explosive experiments with porous silicon ($\rho_0 = 10^3$ kg/m$^3$). The obtained pressure dependence of the conductivity is characterized by saturation at high pressures. Careful analysis of the oscillograms showed that to within 5 nsec the conductivity appears at the moment the SW emerges into the sample and remains constant behind the shockwave throughout the entire observation time. For comparison, Fig. 2 shows the measurements of the electric conductivity of silicon whose density is close to the starting value; the measurements were performed by Japanese investigators (curve 2) [25]. In this work we employed a measurement cell in which the shunt and sample were spatially separated. For low pressures ~3 GPa our measurements are virtually identical to those of [25]. At high pressures (~10 GPa), however, the values of the conductivity measured by our method are an order of magnitude higher and constitute ~$10^6$ $\Omega^{-1} \cdot m^{-1}$. We believe that this discrepancy is attributable to the poor time resolution of the cell with the removal shunt, which turned out to be longer than the time over which the high pressure is maintained in the sample studied. A series of experiments performed with single-crystalline silicon (dots on curve 3) turned out to be a unique test for the proposed measurement method. The results show that the electric conductivity grows steeply and reached a plateau at pressures above 12 GPa. This behavior is characteristic for a semiconductor–metal phase transition under compression [29]. For comparison, Fig. 2 shows the computed dependence σ(p) (curve 4) and the experimental points obtained in dynamic experiments in the region of elastic deformations [30], as well as the results of static measurements (curve 5) [31]. Our results show that 1) under dynamic conditions the transition into the conducting state occurs earlier (at lower pressures), 2) in the case of equal pressures the conductivity of the shock-compressed material is higher than under quasistatic compression, but 3) the maximum electric conductivity is two to three times lower than in the static case. This behavior of the dependence σ(p) in the region of the transition can be attributed to shock-induced heating, while in the region of saturation it can be explained by the high degree of defectiveness

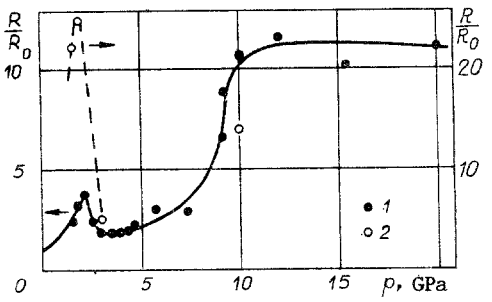


Fig. 3

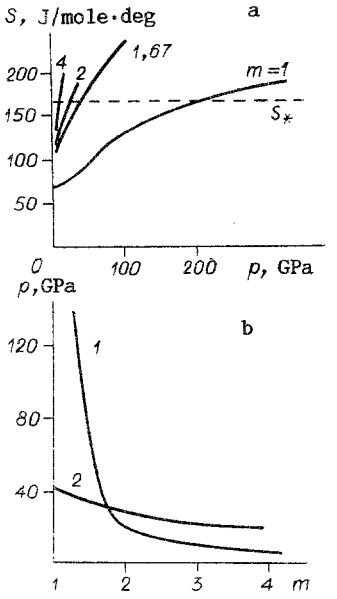


Fig. 4

of the crystalline structure and again by heating of shock-compressed samples. On the whole, however, our results with crystalline silicon agree reasonably well both with existing dynamic experiments at low pressures and static investigations.

5. Our experiments with silicon show that the semiconductor–metal transition with unloading of the sample is reversible. Comparing the oscillograms of the voltage on the measuring cell and the signal from the manganin sensor shows that in the rarefaction wave the sample returns to the low-conductivity state. The time of this transition was determined by the sizes of the shunt and sample, and did not exceed 250 nsec. It turned out that the reverse transition is characterized by significant hysteresis of the conductivity $\sigma(p)$. Starting at the point of the break ($p \approx 12$ GPa) the reverse curve for the single crystal diverges from the loading curve, and the difference in the value of $\sigma$ exceeds an order of magnitude.

6. The proposed method was employed to measure the electric conductivity of powders of a number of metals: aluminum (fine powder and powder), lead, tin, and others. In the starting state all of them are nonconducting. The conductivity under shock compression depends on the starting porosity and the pressure in the wave and is characterized by values of $\sim 5 \cdot 10^5$ $\Omega^{-1} \cdot m^{-1}$ for the fine powder and $\sim 3 \cdot 10^6$ $\Omega^{-1} \cdot m^{-1}$ for the metal powders.

Metal–Semiconductor Phase Transition. In accordance with what was said above, this transition is atypical for high-pressure physics and is observed quite rarely – predominantly in rare-earth elements and their compounds [32-34].

Ytterbium, one of the most interesting members of the lanthanide group, was selected for the experiments. The advantages of ytterbium are that it is comparatively easily available, it can be worked by rolling, and the conductivity changes appreciably under certain compressions [35, 36]. Foil 50-μm thick, which was placed between the Getinaks plates, was employed in the experiment on measuring the electric conductivity. The voltage was measured in the dc regime using a four-point scheme. Two series of experiments with different starting temperatures – 290 and 77 K – were performed. The results obtained are presented in Fig. 3, where the points 1 and the left-hand ordinate scale refer to the starting temperature of 290 K, while the points 2 and the right-hand scale refer to 77 K. The obtained dependence $R(p)/R_0$ agrees qualitatively with the results of [36]. The pressure dependence of the resistance has three characteristic regions: 1) a maximum in the region 1 GPa < p < 3 GPA, 2) a drop in the region 3 GPa < p < 8 GPa; and, 3) growth in the region p > 8 GPa. The maximum of the resistance corresponds to transition of ytterbium into the semiconducting state. Evidence for this is obtained by comparing the results obtained with different starting temperatures. The second section of the dependence R(p) corresponds to the inverse semiconductor–metal transition. Analysis of the phase diagram of ytterbium [37] and evaluation of the resistance for p > 8 GPa is associated with melting of shock-compressed ytterbium. The maximum recorded increase in the resistance of the sample equalled a factor of 25 and is

most likely limited by appreciable shock-induced heating of ytterbium under large compression. Using a complicated system of appropriately selected materials it is possible to transfer from shock compression to practically isoentropic compression, thereby lowering the temperature of the compressed sample and the level of the thermally excited electric conductivity. Two circumstances limit progress along this path. Our measurements of the conductivity of samples compressed with different starting temperatures permitted obtaining for the gap width at a pressure of 2 GPA $\Delta E \approx 0.05$ eV. The comparatively low pressures corresponding to the transition of ytterbium into a semiconductor indicates that the difference of the temperatures of shock-induced and shock-free compression will not be very large, which with a low activation energy will not strongly affect the final conductivity. Since the final temperature of isoentropic compression is proportional to the starting temperature, it is best to perform deep cooling of the sample together with transfer to multistep compression. The second restriction with a transfer to shock-free compression is associated with the increase in the growth time of the pressure and the growth time of the resistance. In our experiments the growth time of the resistance equaled 50 nsec, which corresponded to the time interval over which the pressure is established by the shock wave in the sample, i.e., no delay was observed in the phase transition.

Metal–Vapor Phase Transition in Compression and Unloading Waves. The possibility of the occurrence of a metal–vapor phase transition in the unloading wave was first pointed out in [11]. Analysis of the mutual position of the shock adiabat of the material, the family of unloading isoentropes, and the phase diagram showed that for a normal shock adiabat the loading of the material with a quite strong SW and subsequent unloading led to complete vaporization of the material. It was first noted in [38] that the shock adiabats of highly porous materials lie in the region of specific volumes that are significantly larger than the normal volume of the continuous material, i.e., in the gas-phase region. This means that such materials are vaporized by shock compression. Thus the material can be vaporized in both compression and unloading waves. Whether this happens in the SW or in the rarefaction wave depends on the position of the shock adiabat, i.e., it is determined by the porosity of the material.

We evaluated the conditions of the metal–vapor transition in an SW for a number of materials. For this we employed the entropy criterion formulated in [11] and data on the shock compressibility of materials [16, 39], and in those cases when this information was inadequate we represented the shock adiabat analytically [40]. The temperature was determined based on the growth in the internal energy of the material in the SW and the constant heat capacity. The numerical values of the entropy at the critical point $S_*$ were taken from [41] and the necessary thermodynamic constants and coefficients were taken from [42-45].

An example of the evaluation of the parameters of the metal–vapor transition is given in Fig. 4 for lead. Figure 4a shows the dependence of the entropy of lead on the pressure in the SW S(p), obtained for different values of the porosity m. As m is increased, the pressure in the SW giving rise to vaporization decreases systematically; this is associated with the large thermal heating of the porous material. This dependence is shown by curve 1 in Fig. 4b. The pressure in the SW generated in the material by an explosive (curve 2, the explosive consists of TG 50-50) also drops at the same time. Since curves 1 and 2 drop off at different rates, as one can see from Fig. 4b vaporization is possible for sufficiently porous samples. The values of $m_*$ and $p_*$, corresponding to complete vaporization of a number of metals, are given in Table 2.

The results obtained show that in some highly porous materials a metal–vapor transition should be expected with the use of generally available explosives. Since such a transition leads to the formation of a dense poorly conducting vapor, it is of great interest for use in electrophysical experiments. A promising material in this regard is nickel, since its commercially produced powders are distinguished by a high spectrum of porosities.

## 3. APPLICATION OF INSULATOR–METAL PHASE TRANSITIONS TO THE PROBLEMS OF SWITCHING HIGH CURRENTS

In the last ten years the problem of creating a fast switch has become the central problem in high-current pulsed technology [2-6].

There now exist switches operating on different physical principles: mechanical rupture of a current conductor, electric explosion of a conductor, compression of a plasma channel by an SW, magnetic switch, plasma focus phenomenon, and stimulation of different types of

TABLE 2

| Metal | $m_*$ | $p_*$, GPa |
|---|---|---|
| Pb | 1,7 | 31 |
| Sn | 3,6 | 17 |
| Ni | 3,7 | 19 |
| Zn | 4,4 | 17 |
| Al | >8 | — |

plasma instabilities. High technical parameters have been achieved: switching time of about 1 μsec and currents ranging from several to tens of megaamperes. The switch itself is a unique piece of equipment, almost the most complicated element in the entire electric circuit. The problems, confronting experimental technology, of developing fast switches can be solved to a certain extent by improving existing designs. Another important direction in the improvement of switches is the search for promising switching principles.

Investigations of the conductivity of materials in compression and rarefaction waves have shown that the electric properties of materials change radically over short times ($t \ll 1$ μsec). This fact can be taken as a basis for the development of a fast switch based on a new physical principle – switching by means of insulator–metal phase transitions in an SW.

The advantages of this method of switching over traditional methods are obvious: 1) the current is broken without physical rupture of the circuit, so that conditions for arcing do not arise; 2) the elimination of air gaps next to the current conductors ensures high electric strength on switching; 3) the switching time is determined by the passage time of the wave along the sample and can be quite short (tens of nanoseconds for thin samples); and, 4) the switch based on a phase transition enables two operators: switching the current on and off.

All transitions studied above can be employed for purposes of switching. Thus, when silicon in an SW is employed as the working material it is transformed into a metallic state with high electric conductivity and when the sample is unloaded it undergoes the reverse transition into a poorly conducting state. In the case of ytterbium the sequence of transitions is reversed.

To study the possibility of making a switch based on a phase transition we performed model experiments with a switch based on powdered silicon. The device included buses connected by a rupturable copper bridge, a long explosive charge, and a 5-mm thick layer of silicon powder. The current in the circuit was generated by discharging a capacitor. At the moment the current reached its maximum value the bridge ruptured and the current was switched into the silicon. After the detonation wave passed through the entire length of the charge the working material was unloaded and the current was switched off. The current equaled 30 kA and was halved within 3 μsec. The resistance of the switch equals $5 \cdot 10^{-3}$ Ω in the closed state and exceeds 4 Ω in the open state. The experiments performed showed that it is in principle possible to make a switch based on phase transitions in an SW. Higher parameters of the switch can be achieved by reducing the thickness of the working material and by replacing the powder with a monolithic material.

The ideal working body for a switch is a superconductor. Under the action of an SW the temperature of such a sample can exceed the critical temperature, and it will transform into a poorly conducting state. This transition is the limiting case of phase transitions of the metal–semiconductor type, studied in Sec. 2. A switch based on a superconductor has all the features of the above-studied switches based on phase transitions and, in addition, it does not have any Joule losses in the closed state. The high-temperature, ceramic-based superconductors which have appeared in the last few years will probably soon make these tempting propositions a reality.

## 4. SHOCK-WAVE COMPRESSION OF MAGNETIC FLUX

A method for compressing magnetic flux with SWs, giving rise to a transition of the material from a nonconducting into a conducting state, was proposed in [46-49] and independently in [50, 51]. The method is based on the creation of a closed configuration consist-

ing of several SWs, which converges to some point and creates in it a strong magnetic field. The conductivity in the material can arise by any of the mechanisms listed in Sec. 1. Shock-wave magnetic cumulation was first realized with a transition of silicon powder into the conducting state [47, 50, 51]. Later it was suggested that powders of metals be employed [48, 49]. The highest compression and magnetic fields were obtained in experiments with fine aluminum powder [52-55].

The fundamental difference between shock-wave compression of magnetic flux from classical magnetic cumulation [56, 57] lies in the fact that when matter is compressed a significant fraction of the flux remains frozen in the conductor formed and is then transferred together with it. This phenomenon is simplest to understand by representing the starting nonconducting material in the form of a collection of extremely small, spatially separated, conducting granules which are so small that the passage time of the SW front across the cross section of the granule is longer than the relaxation time of the magnetic field in it, whence follows a restriction on the particle size $a < 1/\mu_0 \sigma D$.

In this case, compression of the material is accompanied by expulsion of only the fraction of the magnetic flux confined in the space between the conducting particles into the region in front of the SW front, and the remaining flux is irretrievably lost. It is obvious that the losses are determined by the degree of porosity of the starting material, i.e., by the ratio of the starting density $\rho_0$ to the density $\rho_*$ of the conducting phase — the smaller the compression of the material ($\rho_0/\rho_* \sim 1$) the smaller the pores, the larger the losses, and the smaller the degree of increase of the magnetic field with fixed geometric compression of the region with the trapped magnetic flux are [53, 54]. Regardless of how paradoxical it appears at first glance, however, appreciable losses of flux which are inherent to the shock-wave method of magnetic-flux compression create definite positive effects. First, systematic freezing-in of the magnetic field in the conductor created by the traveling SW is accompanied by the appearance of a quite smooth distribution of the field in the moving material. As a result, the current layer in the conducting material turns out to be thick, the current density is low, and the associated overheating of the material and development of magnetohydrodynamic instabilities are substantially weaker than in the classical magnetic-cumulation schemes. In addition, the large thickness of the current layer leads to more efficient extraction of energy from a large volume of the moving material. The second positive effect occurs owing to the fact that, for moderate or low compressibility ($\rho_0/\rho_* > 0.5$) the shedding of flux into the conducting material is so large that the total energy of the magnetic field in the material and in front of the SW turns out to be finite even with complete compression of the region with the trapped magnetic flux. This opens up the possibility of operating with large changes in the transverse dimensions of the region with the magnetic field under conditions of limited initial energy, and the phenomenon of hydrodynamic cumulation accompanying motion of the compressed material to the axis can be employed in the axisymmetric case and high mechanical and, as a consequence, magnetic energy densities can be achieved [53, 54]. Restrictions of the possible amplification of the field in this case appear owing to the finite electric conductivity of the material in the compressed state. For limiting compression of the field in the axisymmetric case a very optimistic (in the light of the data on the electric conductivity) estimate

$$\beta_* \sim \exp\left(\frac{1}{2}\,\mathrm{Re}_m \frac{\rho_0}{\rho_*}\right),$$

where $\mathrm{Re}_m = \mu_0 \sigma D_0 r_0$ is the magnetic Reynolds number, $D_0$ is the starting velocity of the SW, and $r_0$ is the initial radius of the region of compression, can be obtained.

The achievement of the limiting amplification of the field $\beta_*$ is predicted theoretically for complete convergence of the compressing SWs to the axis. In practice, the possibilities of maximum compressions are limited by the transverse dimensions of the sensors employed for the measurements. Numerical modeling of the problem showed that the maximum recorded magnetic flux depends strongly on the starting field, the degree of compressibility of the material accompanying the transition into the conducting state, and the starting dimensions of the experimental system. The highest, experimentally recorded amplification of the field equaled a factor of 90, while the magnitude of the field reached 350 T.

The method of compression of magnetic flux in a material that is transferred under compression into a conducting state opens up a number of new possibilities for obtaining extreme energy densities and physical experiments associated with them. The use of several

discrete elements of this type in the experiments performed by A. I. Pavlovskii and his coworkers made it possible to prevent catastrophic mixing of the field with the material of the cumulating conducting shell, stabilize the compression of the field, and achieve an outstanding result – 1200 T in a reproducible experiment [58, 59]. The development of special metal–insulator composite materials with a programmed level of compression for the transition into the conducting state is one of the promising directions for future work on increasing energy cumulation.

## LITERATURE CITED


1. The Physics of High Energy Density, P. Caldirola and H. Knoepfel (eds.), Academic Press, New York (1967).
2. "Megagauss physics and technology," in: Proc. 2nd Int. Conf. on Megagauss Magnetic Field Generation and Related Topics, Washington, 1979, New York (1980).
3. "Superstrong magnetic fields. Physics, technology, and applications," in: Proceedings 3rd Int. Conf. on the Generation of Megagauss Magnetic Fields and Related Experiments, Novosibirsk, 1983, Nauka, Moscow (1984).
4. "Megagauss technology and pulsed power applications," in: Proc. 4th Int. Conf. on Megagauss Magnetic Field Generation and Related Topics, Santa Fe, 1986, New York–London (1987).
5. Accumulation and Switching of Energy at High Energy Densities [Russian translation], Mir, Moscow (1979).
6. E. P. Velikhov (ed.), Physics and Technology of Powerful Pulsed Systems [in Russian], Énergoatomizdat, Moscow (1987).
7. B. A. Larionov, F. M. Spevakova, A. M. Stolov, et al., "Problems of accumulation and conversion of electromagnetic energy in pulsed power supply systems with inductive storage," in: Physics and Technology of Powerful Pulsed Systems [in Russian], E. P. Velikhov (ed.), Énergoatomizdat, Moscow (1987).
8. P. W. Bridgman, The Latest Works in the Field of High Pressures [Russian translation], IL, Moscow (1948).
9. Solids Under High Pressures [Russian translation], Mir, Moscow (1966).
10. A. Jayaraman, "Diamond anvil cell and high-pressure physical investigations," Rev. Mod. Phys., 55, No. 1 (1983).
11. Ya. B. Zel'dovich and Yu. P. Raizer, The Physics of Shock Waves and High-Temperature Hydrodynamic Phenomena [in Russian], Fizmatgiz, Moscow (1963).
12. L. V. Al'tshuler, "Application of shock waves in high-pressure physics," Usp. Fiz. Nauk, 85, No. 2 (1965).
13. R. Kiler, "Electric conductivity of condensed media at high pressures," in: The Physics of High Energy Densities [Russian translation], Mir, Moscow (1974).
14. G. E. Duvall and R. A. Graham, "Phase transitions under shock-wave loading," Rev. Mod. Phys., 49, No. 3 (1977).
15. L. Davison and R. A. Graham, "Shock compression of solids," Phys. Rep., 55, No. 4 (1979).
16. R. MacQueen, S. Marsh, J. Taylor, et al., "Equation of state of solids based on the results of investigations of shock waves," in: Fast Shock Phenomena [Russian translation], Mir, Moscow (1973).
17. D. L. Styris and G. E. Duvall, "Electric conductivity of materials under shock compression (review)," High Temp.–High Press., 2, No. 5 (1970).
18. A. P. Ershov, P. I. Zubkov, and L. A. Luk'yanchikov, "On measurements of the electric conductivity profile on the front of detonation of condensed explosives," Fiz. Goreniya Vzryva, No. 6 (1974).
19. G. I. Kanel', "Application of manganin sensors for measuring the pressure under conditions of shock compression of condensed media," Preprint OIKhM, Chernogolovka (1973).
20. V. V. Yakushev, "Electrical measurements in a dynamic experiment," Fiz. Goreniya Vzryva, No. 2 (1978).
21. A. A. Brish, M. S. Tarasov, and V. A. Tsukerman, "Electric conductivity of dielectrics in strong shock waves," Zh. Éksp. Teor. Fiz., 38, No. 1 (1960).
22. L. V. Kuleshova, "Electric conductivity of boron nitride, potassium chloride, and Teflon behind the front of a shock wave," Fiz. Tverd. Tela, 11, No. 5 (1969).
23. S. S. Nabatov, A. N. Dremin, V. I. Postnov, et al., "Measurements of the electric conductivity of sulfur under dynamic compression up to 400 kbar," Pis'ma Zh. Tekh. Fiz., 5, No. 3 (1979).
24. V. I. Postnov, L. A. Anan'eva, A. N. Dremin, et al., "Electrical conductivity and compressibility of sulfur under shock compression," Fiz. Goreniya Vzryva, No. 4 (1986).

25. T. Mashimo, Y. Kimura, and K. Nagayama, "Precise measurement of the electrical conductivity of silicon under shock compression," Kumamoto University (1984).
26. B. Aller, "Physical experiments with strong shock waves," in: Solids Under High Pressures [Russian translation], Mir, Moscow (1966).
27. S. D. Gilev and A. M. Trubachev, "Measurement of high conductivity of silicon in shock waves," in: Abstracts of Reports at the All-Union School-Seminar on Fundamental Problems of the Physics of Shock Waves, Vol. 1, Part 1, Chernogolovka (1987).
28. S. D. Gilev and A. M. Trubachev, "Measurement of high electrical conductivity of silicon in shock waves," Zh. Prikl. Mekh. Tekh. Fiz., No. 6 (1988).
29. S. Minomura and H. G. Drickamer, "Pressure induced phase transitions in silicon, germanium, and some III-V compounds," J. Phys. Chem. Solids, 23, 451 (1962).
30. G. Rosenberg, "Resistivity measurements in silicon compressed by shock waves," J. Phys. Chem. Solids, 41, 561 (1980).
31. F. P. Bundy and J. S. Kasper, "Electrical behavior of sodium–silicon clathrates at very high pressures," High Temp.–High Press., 2, 429 (1970).
32. A. A. Bakanova, I. P. Dudoladov, and Yu. M. Sutulov, "Electronic transitions in hafnium, europium, and ytterbium at high pressures," Fiz. Tverd. Tela, 11(7) (1969).
33. N. F. Mott, Metal–Insulator Transitions [Russian translation], Nauka, Moscow (1979).
34. H. G. Drickamer and C. W. Frank, Electronic Transitions and the High-Pressure Chemistry and Physics of Solids, Halsted Press, New York (1973).
35. D. B. McWhan, T. M. Rice, and P. H. Schmidt, "Metal–semiconductor transition in ytterbium and strontium at high pressure," Phys. Rev., 177, No. 3 (1969).
36. M. N. Pavlovskii, "Electrical resistance of shock-compressed ytterbium," Zh. Éksp. Teor. Fiz., 73, No. 1 (1977).
37. W. J. Carter, J. N. Fritz, S. P. Marsh, et al., "Hugoniot equation of state of the lanthanides," J. Phys. Chem. Solids, 36, 741 (1975).
38. Yu. B. Khvostov, "Study of the physics of shock waves in porous materials," Rep. Inst. Fiz. Zemli Akad. Nauk SSSR, Moscow (1984).
39. K. P. Stanyukovich (ed.), Physics of Explosions [in Russian], Nauka, Moscow (1975).
40. G. A. Simons and H. H. Legner, "An analytical model for the shock Hugoniot in porous materials," J. Appl. Phys., 53, No. 2 (1982).
41. V. E. Fortov, A. N. Dremin, and A. A. Leont'ev, "Evaluation of critical point parameters," Teplofiz. Vys. Temp., 13, No. 5 (1975).
42. V. N. Yurepev and P. D. Lebedev (eds.), Handbook of Heat Engineering [in Russian], Vol. 1, Énergiya, Moscow (1975).
43. C. Kittel, Introduction to Solid State Physics, Wiley, New York (1971).
44. I. K. Kikoin (ed.), Handbook of the Tables of Physical Quantities [in Russian], Atomizdat, Moscow (1976).
45. V. P. Glushko et al. (eds.), Handbook of the Thermal Constants of Materials [in Russian], VINITI, Moscow (1970).
46. E. I. Bichenkov, N. G. Skorobogatykh, and A. M. Trubachev, "Magnetic cumulation generator," USSR Inventor's Certificate No. 762,706; Byull. Izobret., No. 1 (1982).
47. E. I. Bichenkov, S. D. Gilev, and A. M. Trubachev, "Magnetic cumulation generator employing the transition of a semiconductor material into a conducting state," Zh. Prikl. Mekh. Tekh. Fiz., No. 5 (1980).
48. S. D. Gilev and A. M. Trubachev, "Production of strong magnetic fields by shock waves in matter," Pis'ma Zh. Tekh. Fiz., 8(15) (1982).
49. S. D. Gilev and A. M. Trubachev, "Production of strong magnetic fields by magnetic cumulation generators based on a porous material," Zh. Prikl. Mekh. Tekh. Fiz., No. 5 (1983).
50. K. Nagayama, "New method of magnetic flux compression by means of the propagation of shock-induced metallic transition in semiconductors," Appl. Phys. Lett., 38, No. 2 (1981).
51. K. Nagayama, T. Oka, and T. Mashimo, "Experimental study of a new mechanism of magnetic flux cumulation by the propagation of shock-compressed conductive region in silicon," J. Appl. Phys., 53, No. 4 (1982).
52. E. I. Bichenkov, S. D. Gilev, and A. M. Trubachev, "Shock-wave magnetic cumulation generators," in: Superstrong Magnetic Fields: Proc. 3rd Int. Conf. on the Generation of Megagauss Magnetic Fields, Nauka, Moscow (1984).
53. E. I. Bichenkov, S. D. Gilev, A. M. Riabchun, et al., "Shock wave method for generation of megagauss magnetic fields," in: Megagauss Technology and Pulsed Power Application: Proc. 4th Int. Conf. on Megagauss Magnetic Field Generation, New York (1987).

54. E. I. Bichenkov, S. D. Gilev, A. M. Ryabchun, et al., "Shock-wave method of generation of megagauss magnetic fields," Zh. Prikl. Mekh. Tekh. Fiz., No. 3 (1987).
55. K. Nagayama and T. Mashimo, "Explosive-driven magnetic flux cumulation by the propagation of shock compressed conductive region in highly porous metal powders," J. Appl. Phys., 61, No. 10 (1987).
56. A. D. Sakharov, R. Z. Lyudaev, E. I. Smirnov, et al., "Magnetic cumulation," Dokl. Akad. Nauk SSSR, 165, No. 1 (1965).
57. C. M. Fowler, R. S. Caird, and W. B. Carn, "Production of very high magnetic fields by explosion," J. Appl. Phys., 31, No. 3 (1960).
58. A. I. Pavlovskii, N. P. Kolokol'chikov, M. I. Dolotenko, et al., "Cascade magnetic cumulation generator of superstrong magnetic fields," in: Superstrong Magnetic Fields: Proc-3rd Int. Conf. on the Generation of Megagauss Magnetic Fields, Nauka, Moscow (1984).
59. A. I. Pavlovskii, A. I. Bykov, M. I. Dolotenko, et al., "Limiting value of reproducible magnetic field in cascade generator MC-1," in: Megagauss Technology and Pulsed Power Applications: Proc. 4th Int. Conf. on Megagauss Magnetic Field Generation, New York (1987).

# STRUCTURE AND DYNAMICS OF A PLASMA PISTON IN RAIL-GUN ACCELERATORS FOR SOLID OBJECTS

A. G. Anisimov, Yu. L. Bashkatov, and G. A. Shvetsov

UDC 538.4+533.95

In recent years, beginning with [1], investigators have paid considerable attention to the study of possible acceleration of dielectric solids by a plasma piston in rail-gun accelerators. One expects that this development process will remove the thermal limits on the speed of metal particles and obtain speeds considerably exceeding the experimental level achieved [2]. Papers have appeared whose authors have considered the possibility of, and discussed plans for equipment to accelerate particles of mass on the order of a gram to speeds of 12 [3], 15 [4, 5], 20 [6, 7], 25[4, 6, 8], 50 km/sec [9], etc. However, it should be noted that, in spite of almost a decade since the publication of [1] and considerable efforts, there has been no substantial progress in the technology of obtaining high speeds. The experimental results are very modest and are at the level of those of [1].

At present it is generally accepted that the main causes limiting the attainment of high speed of macroparticles in rail-gun accelerators with a plasma piston are associated with erosion of the channel walls under the action of the high-power heat flux from the moving plasma piston and the current flowing in the circuit. Analysis of the critical gas density for which the surface temperature of the electrodes reaches the melt temperature shows [10] that one cannot achieve efficient acceleration of the body and avoid erosion of the electrodes. The effect of erosion of the electrodes is different. The presence of added mass leads to the appearance of "limiting" values of the speed of the accelerated particle independently of the mechanism of erosion [10], to redistribution of current in the plasma piston, and to separation of the latter from the accelerated body [11]. Among the causes

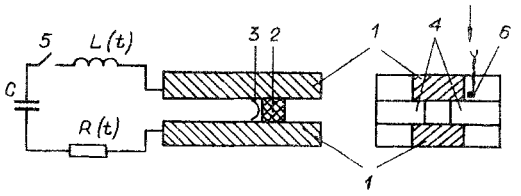


Fig. 1

Novosibirsk. Translated from Zhurnal Prikladnoi Mekhaniki i Tekhnicheskoi Fiziki, No. 2, pp. 145-150, March-April, 1989. Original article submitted August 4, 1988.

0021-8944/89/3002-0303$12.50 